Supporting Information

A smart electrolyte-replenishing semi-dry electrode based on a temperature-responsive hydrogel for sustainable electrophysiological signal acquisition

Yiming Cai[a], Fushuai Wang[a], Lang Yang[c], Lin Chen[c], Jialei Ying[b], Zhenzhong Liu[b], Guozheng Wang[b,d], Chunxin Ma[b,c] and Jun Liu[a,c,*]

a. Key Laboratory for Biomedical Engineering of Education Ministry, Department of Biomedical Engineering, Zhejiang University, Hangzhou, 310027, China

b. Taizhou Key Laboratory of Medical Devices and Advanced Materials, Taizhou Institute of Zhejiang University, Taizhou 318000, China

c. State Key Laboratory of Marine Resource Utilization in South China Sea, School of Chemistry and Chemical Engineering, Hainan University, Haikou 570228, China

d. Department of Sports Science, College of Education, Zhejiang University, Hangzhou 310058, China

Supporting Figures

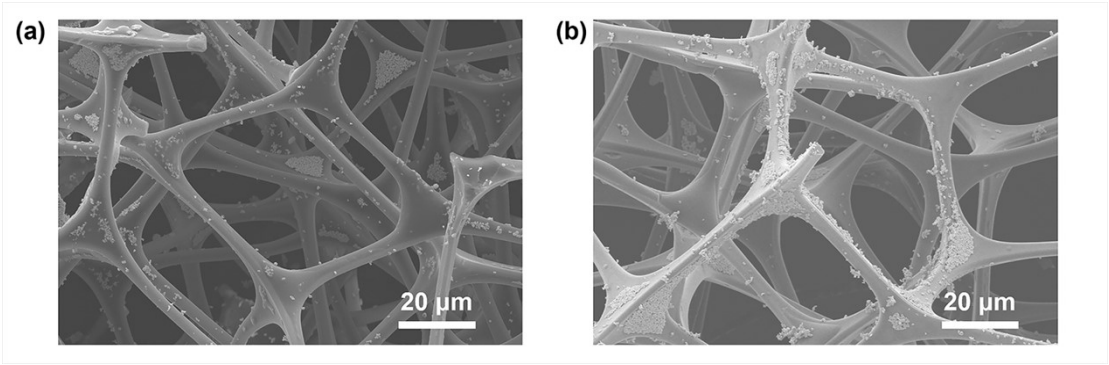

Figure S1. The SEM images of rare sponge immersed in (a) 10% Ag nanoparticles dispersion and (b) 30% Ag nanoparticles dispersion.

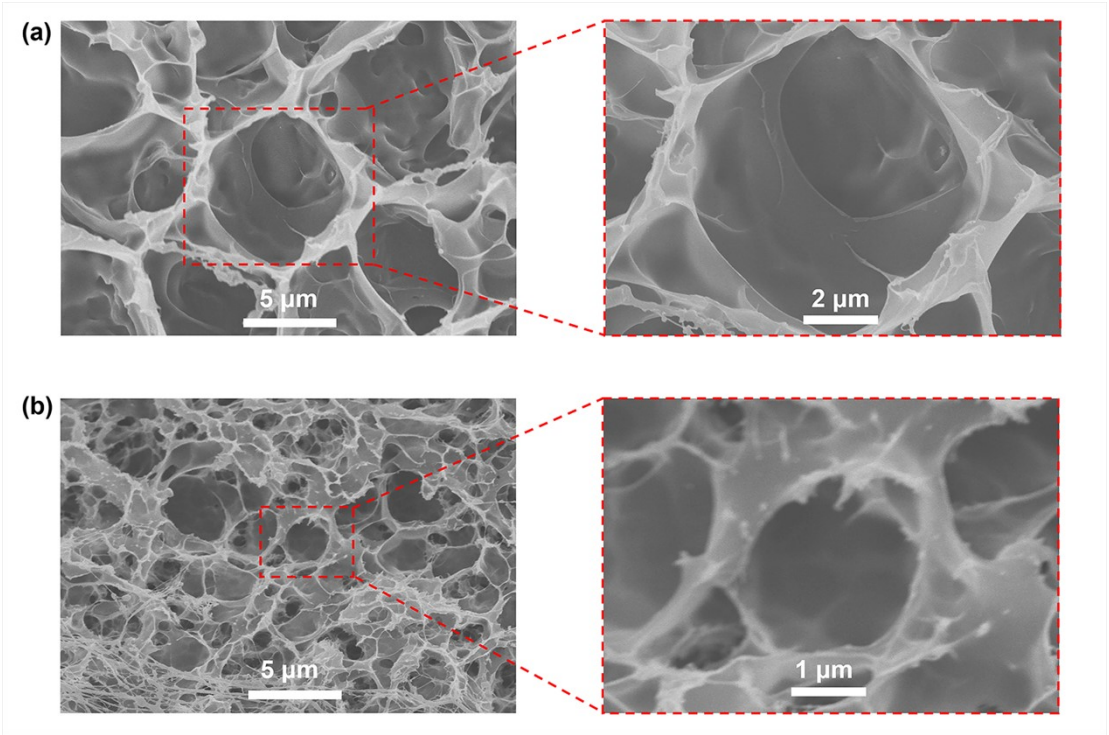

Figure S2. The SEM images of (a) PNIPAM hydrogel and (b) PNIPAM/PVA hydrogel.

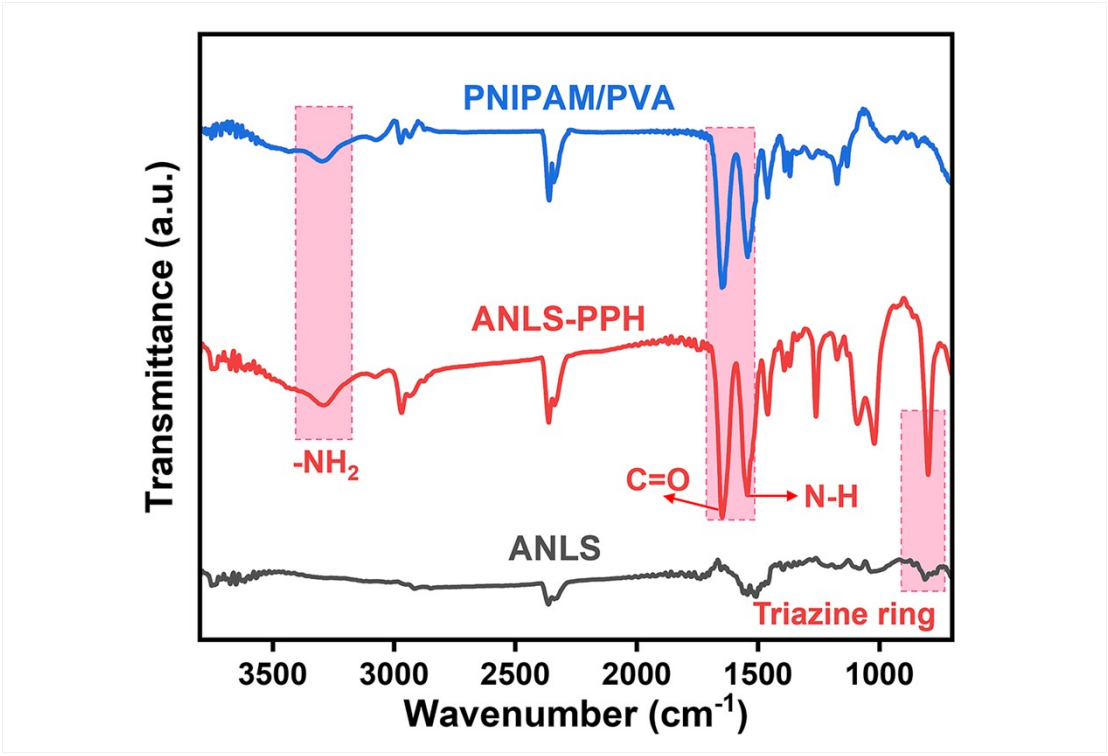

Figure S3. The FT-IR spectra of ANLS, PNIPAM/PVA hydrogel and ANLS-PPH.

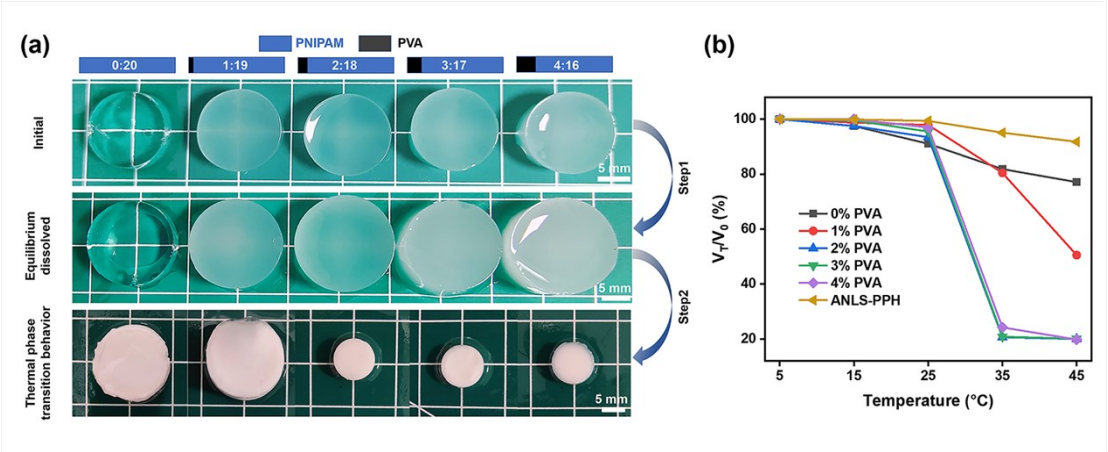

Figure S4. (a) Photographs of hydrogels with different PNIPAM and PVA contents in the original, full swelling and thermal phase transition behavior form. (b) Volume change curves of ANLS-PPH and hydrogels with different PNIPAM and PVA contents under temperature change.

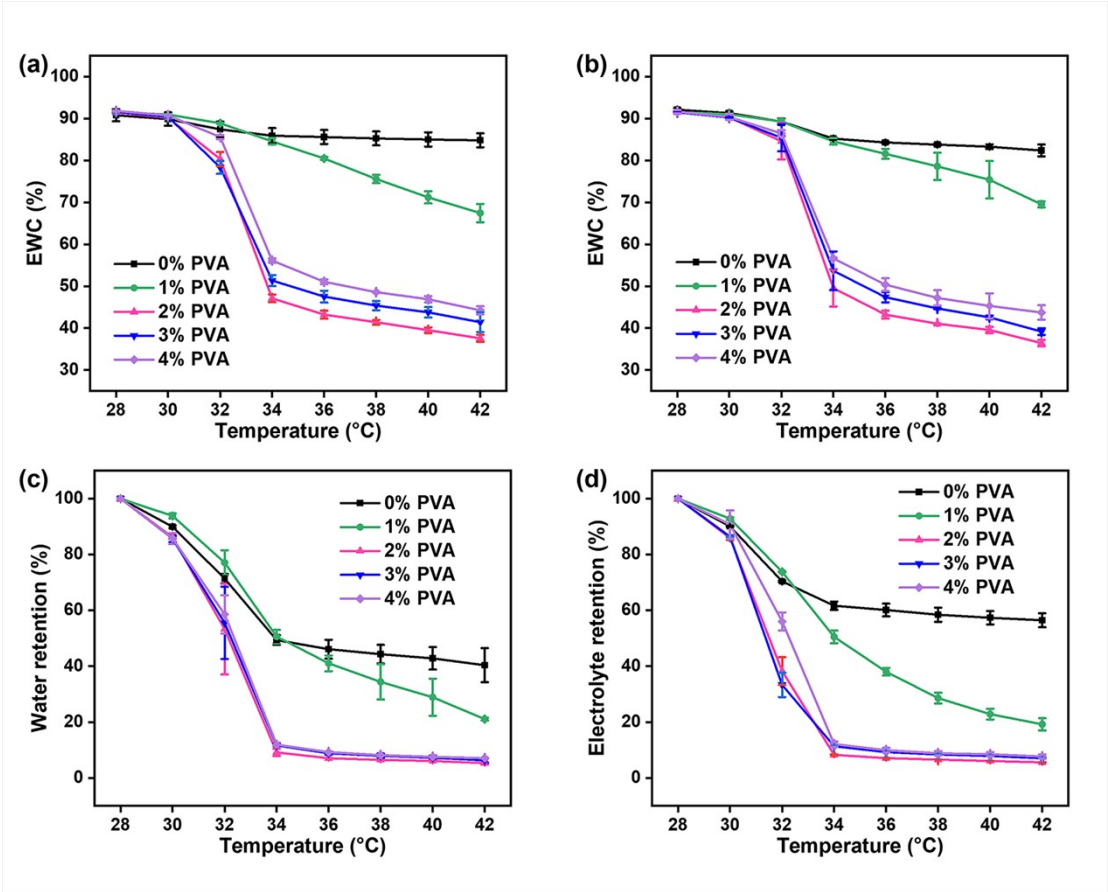

Figure S5. Equilibrium water content-temperature curves of hydrogels with different PVA contents in (a) deionized water and (b) 0.2 mol/L NaCl. Water retention-temperature curves of hydrogels with different PVA contents in (c) deionized water and (d) 0.2 mol/L NaCl.

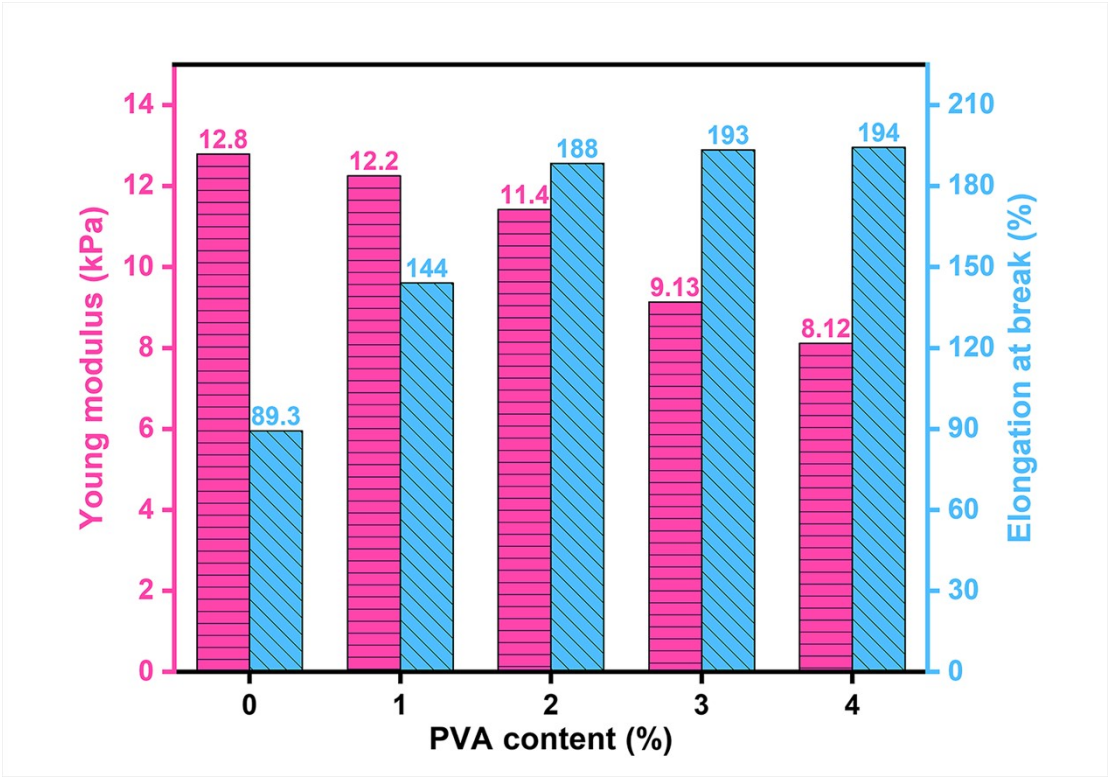

Figure S6. Comparison of the tensile strengths of hydrogels with different PVA contents.

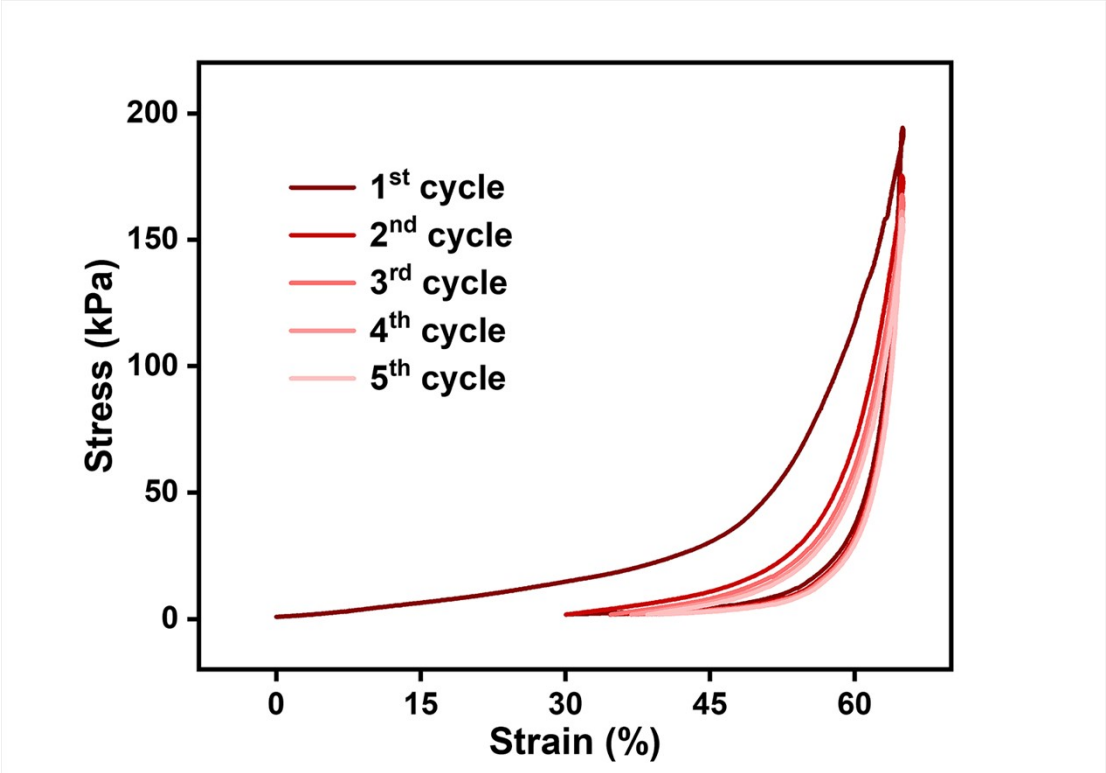

Figure S7. Cyclic compression loading-unloading curves of ANLS-PPH with different cycle times at the same strain.

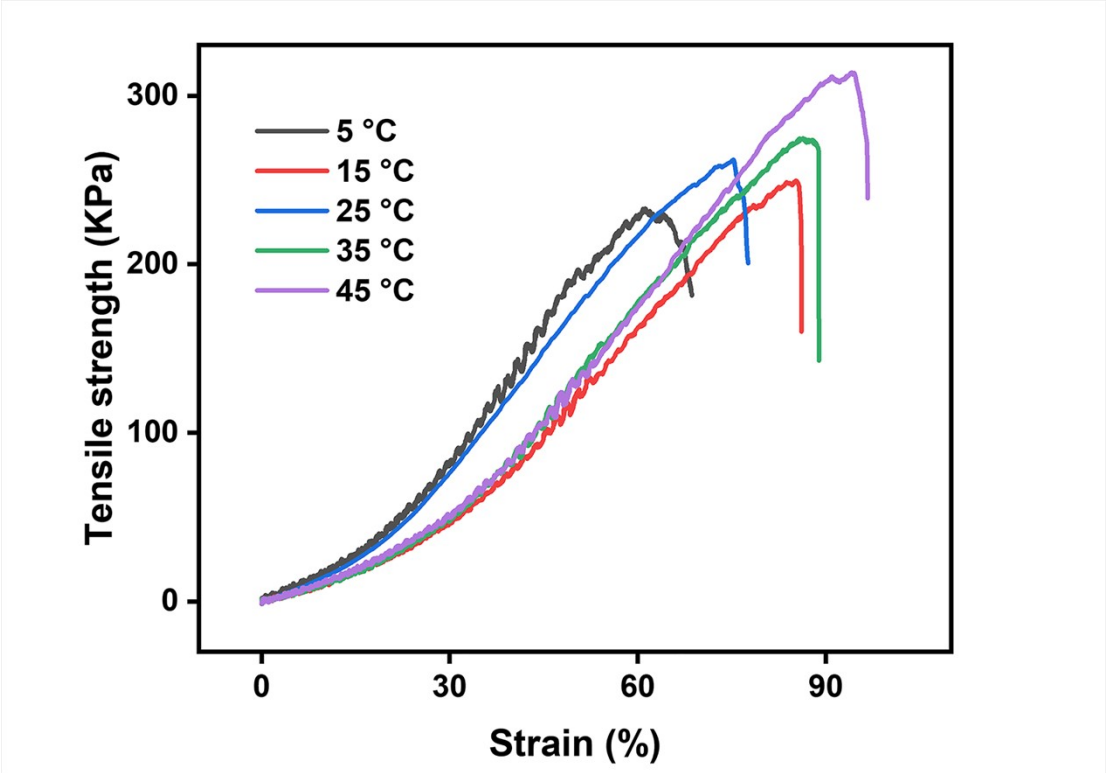

Figure S8. Comparison of tensile strength of ANLS-PPH at different temperatures.

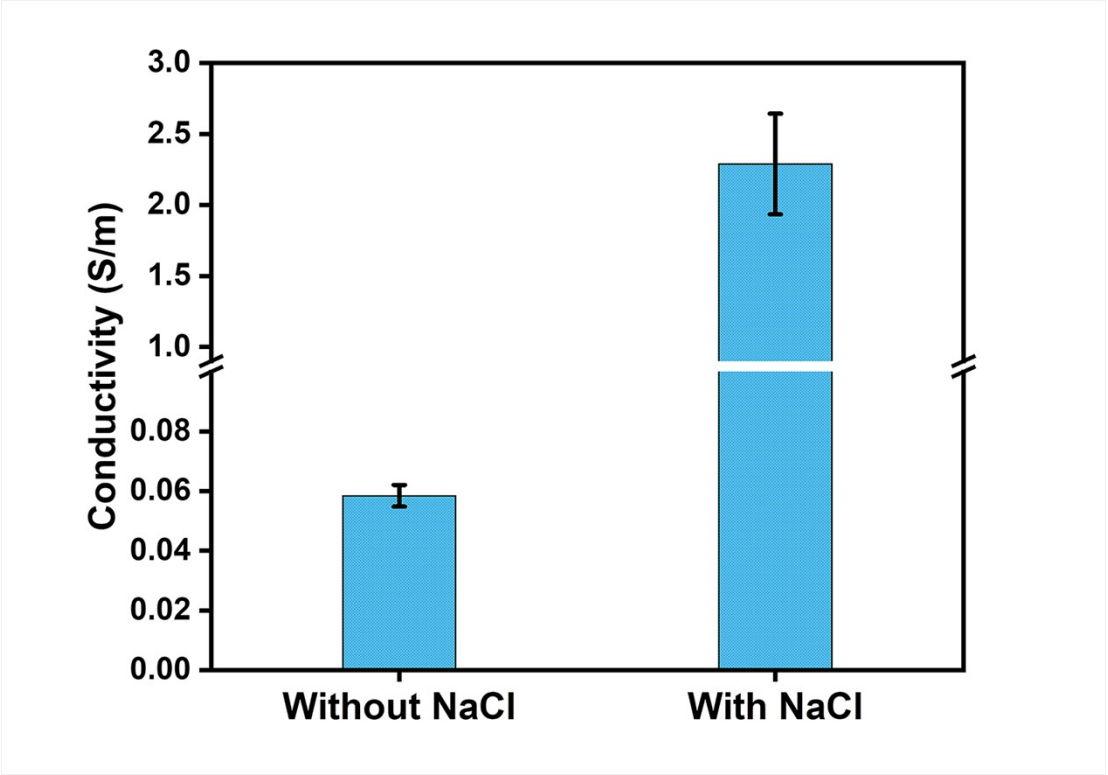

Figure S9. The conductivity for ANLS-PPH without NaCl and with NaCl.

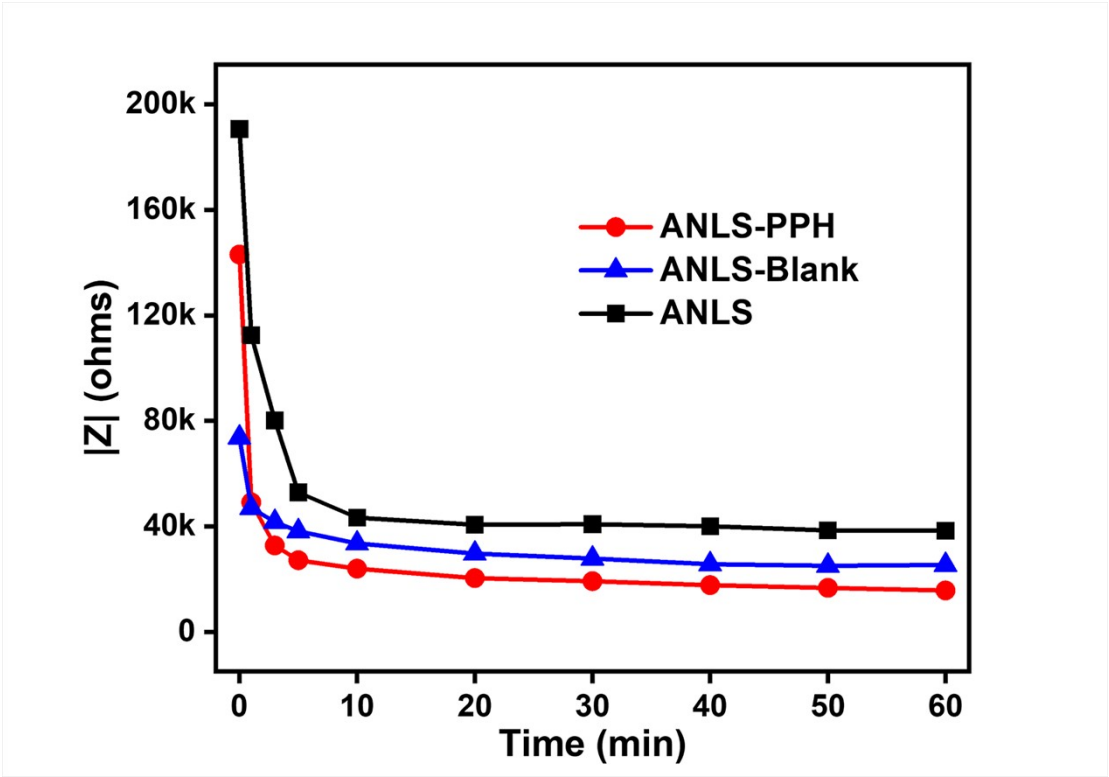

Figure S10. The skin-electrode contact impedance between the ANLS, ANLS-Blank and ANLS-PPH over 1 h.

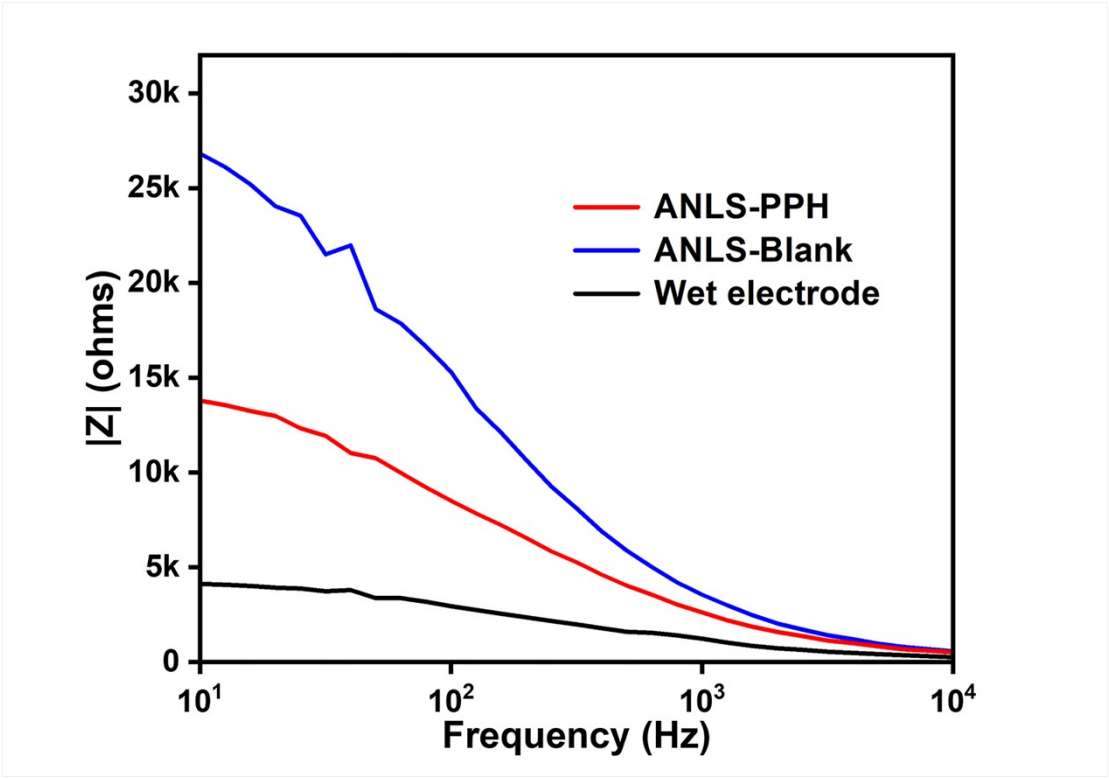

Figure S11. The mean skin-electrode contact impedance spectra of different subjects with ANLS-PPH, ANLS-Blank and wet electrodes.

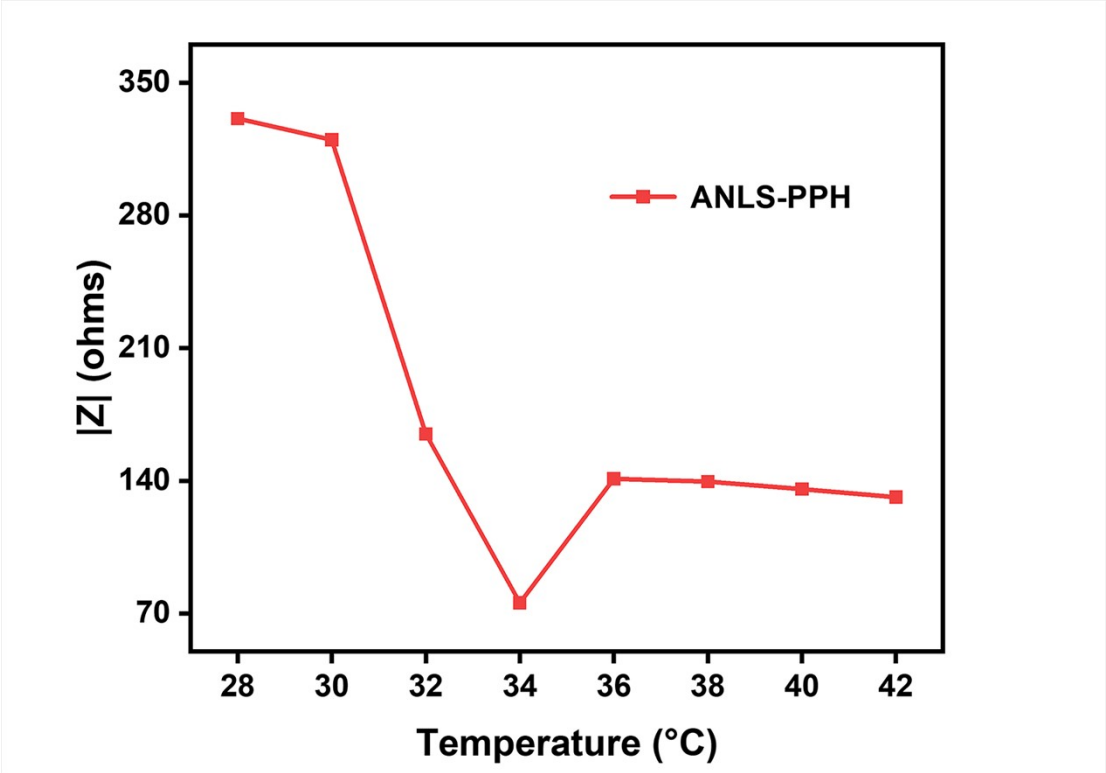

Figure S12. The impedance of ANLS-PPH electrode pairs at different temperatures

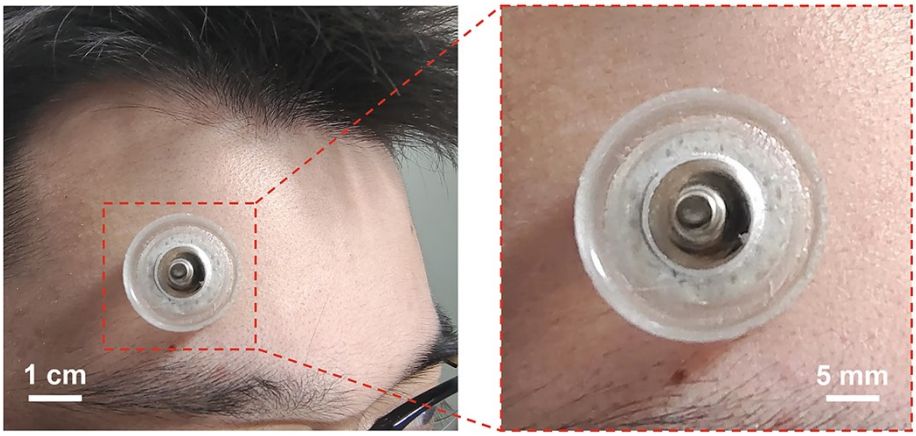

Figure S13. Photographs of the semi-dry electrode located on forehead.

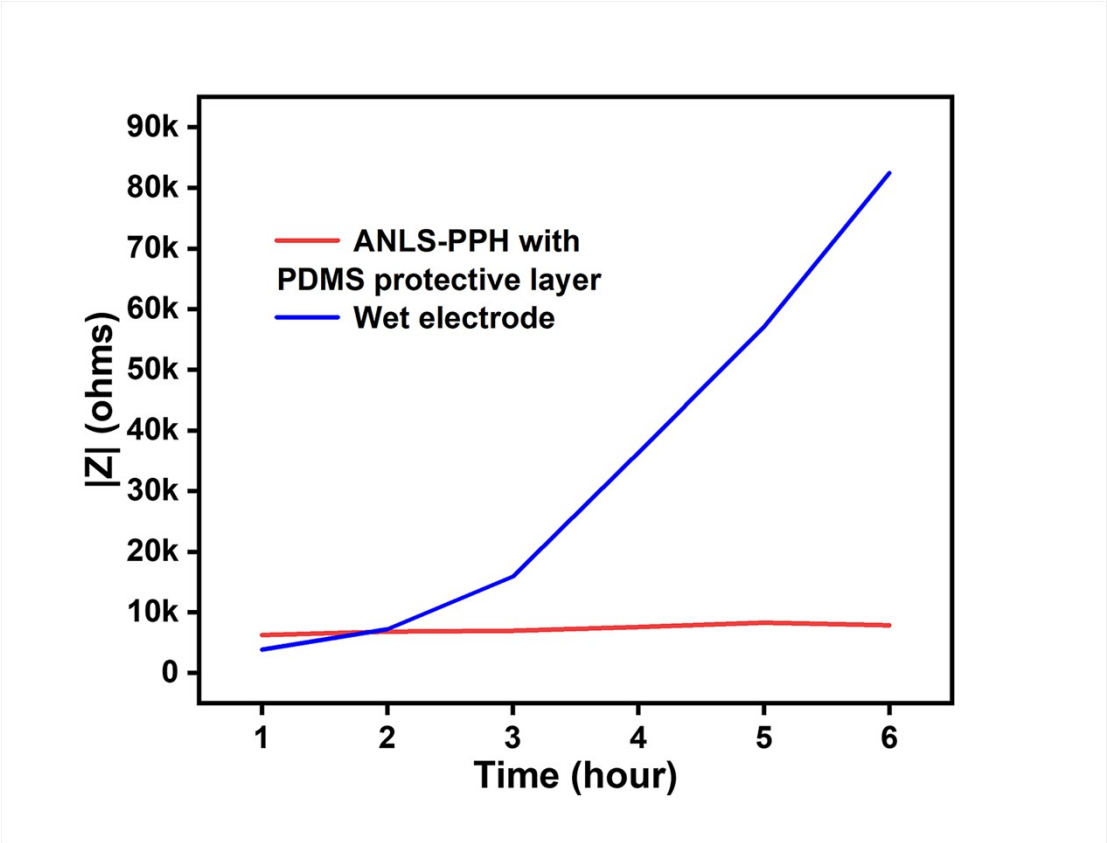

Figure S14. Impedance data for semi-dry and wet electrodes over a period of 6 hours.

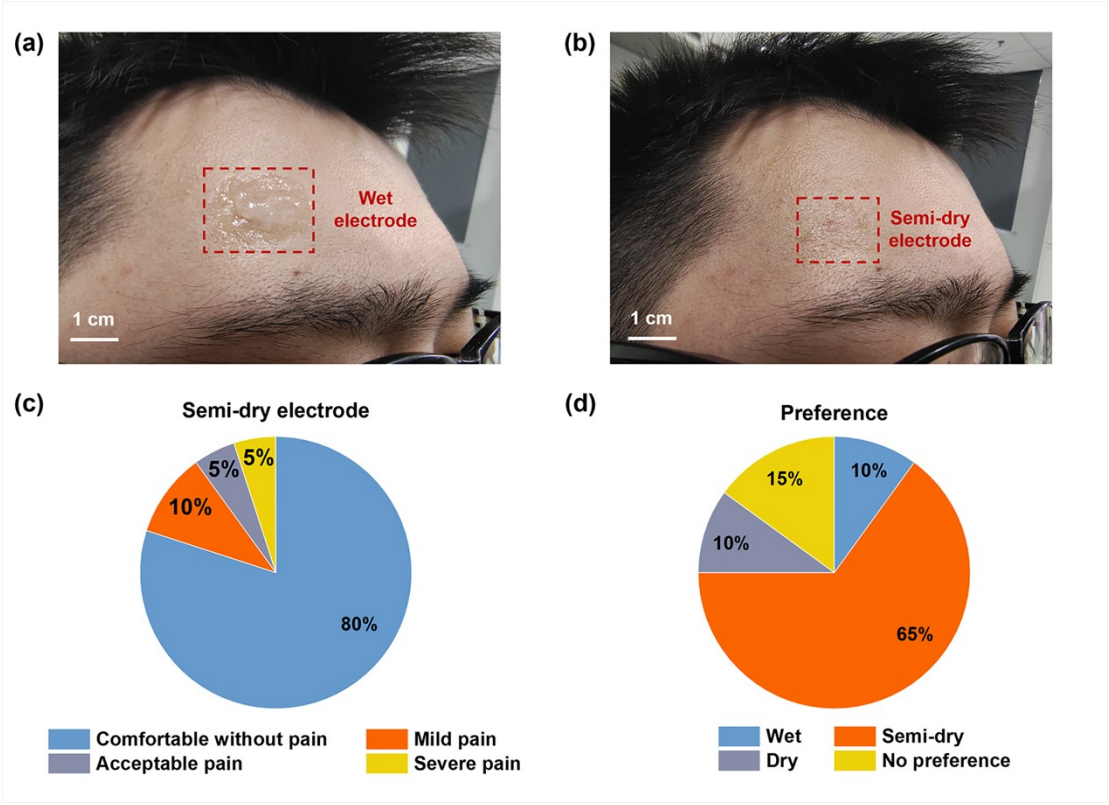

Figure S15. The skin states after experiments of (a) the wet electrode and (b) the semi-dry electrode. (c) Comfort assessment of this semi-dry electrode by different volunteers. (d) Preferences of volunteers for the three types of electrodes.

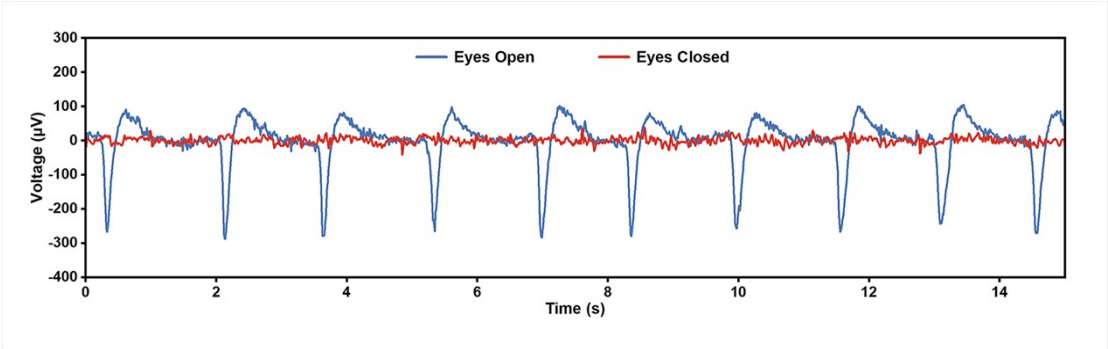

Figure S16. One channel EEG signal recorded by the wet electrode during eyes open and eyes closed.

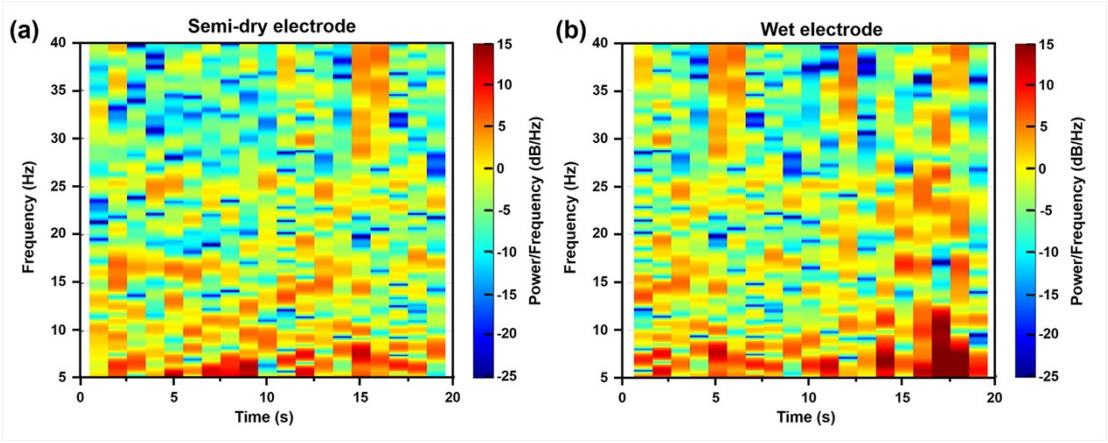

Figure S17. Time-frequency analysis of 0.5-40 Hz signals recorded by (f) the semi-dry electrode and (g) wet electrode with eyes open.

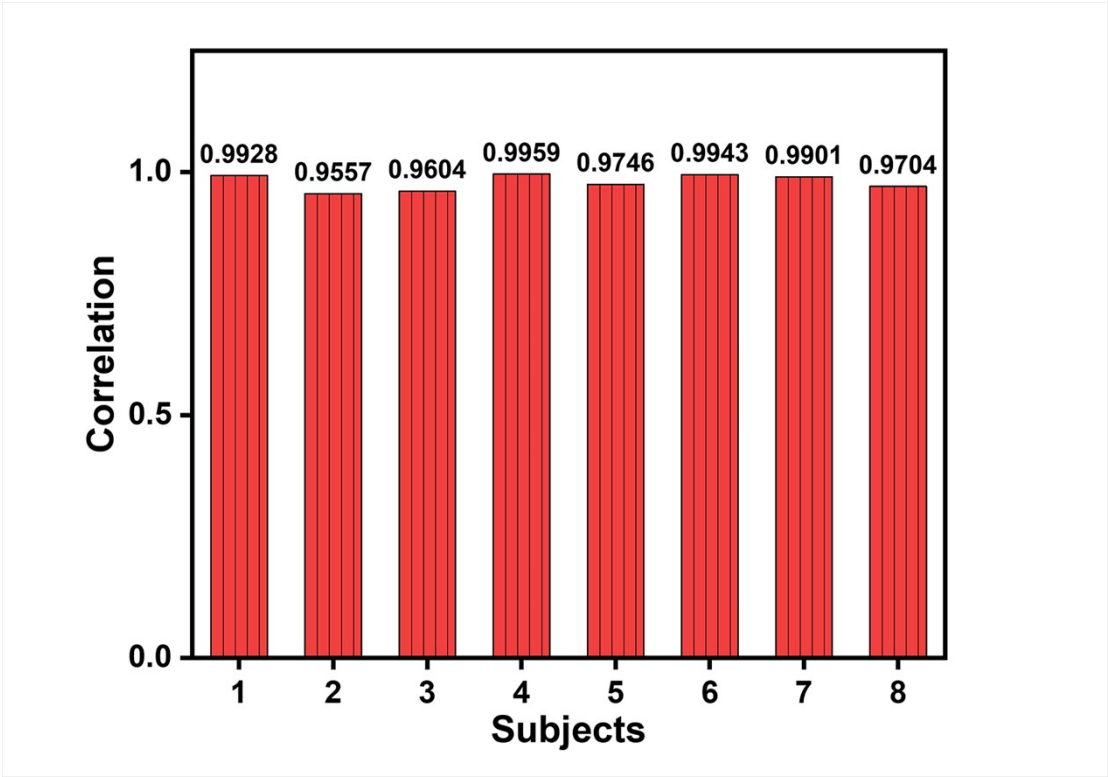

Figure S18. The spectral correlation of signals recorded by the semi-dry electrode and wet electrode.

Supporting Tables

Table S1: Synthesis of PNIPAM hydrogel and PNIPAM/PVA hydrogels by varying the mass concentration of PVA solution.

Hydrogels	PVA (g)	NIPAM (g)	BIS (g)	TEMED (μL)	APS (g)	H_2O (mL)
0% PVA	0	2.0	0.02	50	0.016	12.4
1% PVA	0.1	1.9	0.02	50	0.016	12.4
2% PVA	0.2	1.8	0.02	50	0.016	12.4
3% PVA	0.3	1.7	0.02	50	0.016	12.4
4% PVA	0.4	1.6	0.02	50	0.016	12.4

Table S2: The fitting results of equivalent circuit components.

Parameters	R_{ct}	$CPE_e - T$	$CPE_e - P$	R_e	R_s	$CPE_s - T$	$CPE_s - P$	R_{sub}
ANLS-PPH	3794	2.8023 × 1(	0.86629	65.83	7220	1.2574 × 1(	0.76329	105.8
ANLS-Blank	6303	2.3381 × 1(	0.86701	78.16	12432	7.8473 × 1(	0.79802	105.5
Wet electrode	1044	6.8866 × 1(	0.81644	5.64	3267	1.8034 × 1(	0.84033	104.3

Table S3: Comparisons of representative electrodes.

Materials	Electrode types	Application	Comfort level	Long-term durability	Ways to release electrolyte	Contact impedance (10 Hz)	Reference
Conductive metals	Dry	ECG/EMG/ EEG	Hard and potentially skin-damaging	-	Sweating	$> 100\ k\Omega$	-
Conductive paste	Wet	ECG/EMG/ EEG	Highly comfortable but foreign body sensation on the skin	-	-	$< 5\ k\Omega$	-
Ag/AgCl coated PU; saline	Semi-dry	EEG	-	-	Pressure	-	1
PU sponge; electrolyte fluid	Semi-dry	EEG	Better than dry electrode	$8\ h (< 20\ k\Omega)$	Pressure	$10\ k\Omega$~$35\ k\Omega$	2
Porous ceramics; saline	Semi-dry	EEG	Pain (3 subjects); slight pain (17 subjects)	-	Capillary force	$< 30\ k\Omega$	3
Porous ceramics; saline	Semi-dry	EEG	-	Approximately $20\ k\Omega$ increase up to 8 h.	Capillary force	$21.1 \pm 8.2\ k\Omega$~	4
Carrageenan; Glycerin; conductive salt	Semi-dry	EEG	70% of subjects felt comfortable without pain.	$4\ h (< 76\ k\Omega)$	Auto-release (uncontrollable)	$43 \pm 6\ k\Omega$	5
PAM/PVA hydrogel; saline	Semi-dry	ECG/EEG	-	$8\ h (< 38.2 \pm 5.6$	Auto-release (uncontrollable)	$36.4 \pm 16.8\ k\Omega$	6
PDMS; Ag nanoparticle-loaded sponge; PNIPAM/PVA hydrogel	Semi-dry	ECG/EEG	80% of subjects felt comfortable without pain.	$6\ h (< 10\ k\Omega)$	Body temperature response (smart electrolyte-replenishing)	$8\ k\Omega$~$18\ k\Omega$	This work

References

1. A. R. Mota, L. Duarte, D. Rodrigues, A. C. Martins, A. V. Machado, F. Vaz, P. Fiedler, J. Haueisen, J. M. Nóbrega and C. Fonseca, *Sens. Actuators, A*, 2013, **199**, 310-317.
2. X. Xing, W. H. Pei, Y. J. Wang, X. H. Guo, H. Zhang, Y. X. Xie, Q. Gui, F. Wang and H. D. Chen, *Sens. Actuators, A*, 2018, **270**, 262-270.
3. F. Wang, G. L. Li, J. J. Chen, Y. W. Duan and D. Zhang, *J. Neural Eng.*, 2016, **13**, 046021.
4. G. L. Li, D. Zhang, S. Z. Wang and Y. W. Y. Duan, *Sens. Actuators, B*, 2016, **237**, 167-178.
5. W. H. Pei, X. T. Wu, X. Zhang, A. H. Zha, S. Tian, Y. J. Wang and X. R. Gao, *IEEE Trans. Neural Syst. Rehabil. Eng.*, 2022, **30**, 843-850.
6. G. L. Li, Y. Liu, Y. W. Chen, Y. H. Xia, X. M. Qi, X. Wan, Y. Jin, J. Liu, Q. G. He, K. H. Li and J. X. Tang, *Smartmat*, 2023, **5**, e1173.